Modified Critical State Two-Surface Plasticity Model for Sands

Sørensen, Kris Wessel; Nielsen, Søren Kjær; Shajarati, Amir; Clausen, Johan

Publication date:
2012

Document Version
Accepted author manuscript, peer reviewed version

Modified Critical State Two-Surface Plasticity Model for Sands

Kris Wessel Sørensen
Søren Kjær Nielsen
Amir Shajarati
Johan Clausen

ISSN 1901-7278
DCE Technical Memorandum No. 16

AALBORG UNIVERSITY
Department of Civil Engineering

Aalborg University
Department of Civil Engineering
Geotechnical Engineering

DCE Technical Memorandum No. 16

Modified Critical State Two-Surface Plasticity Model for Sands

by

Kris Wessel Sørensen
Søren Kjær Nielsen
Amir Shajarati
Johan Clausen

June 2012

Scientific Publications at the Department of Civil Engineering

Technical Reports are published for timely dissemination of research results and scientific work carried out at the Department of Civil Engineering (DCE) at Aalborg University. This medium allows publication of more detailed explanations and results than typically allowed in scientific journals.

Technical Memoranda are produced to enable the preliminary dissemination of scientific work by the personnel of the DCE where such release is deemed to be appropriate. Documents of this kind may be incomplete or temporary versions of papers—or part of continuing work. This should be kept in mind when references are given to publications of this kind.

Contract Reports are produced to report scientific work carried out under contract. Publications of this kind contain confidential matter and are reserved for the sponsors and the DCE. Therefore, Contract Reports are generally not available for public circulation.

Lecture Notes contain material produced by the lecturers at the DCE for educational purposes. This may be scientific notes, lecture books, example problems or manuals for laboratory work, or computer programs developed at the DCE.

Theses are monograms or collections of papers published to report the scientific work carried out at the DCE to obtain a degree as either PhD or Doctor of Technology. The thesis is publicly available after the defence of the degree.

Latest News is published to enable rapid communication of information about scientific work carried out at the DCE. This includes the status of research projects, developments in the laboratories, information about collaborative work and recent research results.

Published 2012 by
Aalborg University
Department of Civil Engineering
Sohngaardsholmsvej 57,
DK-9000 Aalborg, Denmark

Printed in Aalborg at Aalborg University

ISSN 1901-7278
DCE Technical Memorandum No. 16

Modified Critical State Two-Surface Plasticity Model for Sands

Kris Wessel Sørensen[1] Søren Kjær Nielsen[1] Amir Shajarati[1] Johan Clausen[2]

Department of Civil Engineering, Aalborg University

Abstract

This article describes the outline of a numerical integration scheme for a critical state two-surface plasticity model for sands. The model is slightly modified by LeBlanc (2008) compared to the original formulation presented by Manzari and Dafalias (1997) and has the ability to correctly model the stress-strain response of sands. The model is versatile and can be used to simulate drained and undrained conditions, due to the fact that the model can efficiently calculate change in void ratio as well as pore pressure. The objective of the constitutive model is to investigate if the numerical calculations can be performed with the Forward Euler integration scheme. Furthermore, the model is formulated for a single point.

1 Introduction

With the rapidly growing increase in computational power over the last decades, constitutive models that accurately simulate the stress-strain behaviour of different materials have been used within different engineering fields. However, for granular materials only simple classical plasticity models such as Mohr-Coulomb or Cam-Clay have been widely used in most engineering codes. These models may be sufficient for many simple geotechnical problems, but fail to simulate accurate stress-strain behaviour when dealing with complex problems. Therefore more advanced models are required when dealing with offshore geotechnical problems. Effects from cyclic loading such as accumulation of pore pressure, cyclic liquefaction and cyclic mobility are typically needed to be taken into account.

The framework of Critical State Soil Mechanics (CSSM) developed by Schofield and Wroth (1968) provides a broad framework to explain the fundamental behaviour of different soil materials. Within this framework, Manzari and Dafalias (1997) developed a versatile constitutive model named *Critical State Two-Surface Plasticity Model for Sands*, that is able to model both drained an undrained behaviour of cohesionless soils subjected to cyclic loading. LeBlanc (2008) made modifications to the model by introducing an alternative multi-axial surface formulation based on shape functions used to prescribe a family of smooth and convex contours in the octhahedral plane.

This article outlines the physical aspects of the model proposed by LeBlanc (2008), and seeks to describe the different model parameters. When implementing the constitutive model, a simple integration scheme in form of *Forward Euler* is used instead of the proposed *Return Mapping Method* used by LeBlanc (2008). This is done in order to simplify the calculations and investigate if the accuracy of the model is still preserved.

2 Formulation of Model

The following section describes the modified critical two-surface plasticity model for sands in detail, and has its point of reference in LeBlanc (2008).

2.1 Peak Shear Strength

A dense sand specimen will dilate when sheared and therefore has a larger shear strength due to the increased amount of energy needed in order to get the granular particles to slide over adjacent particles. The peak shear strength described as the upper limit in a stress space, normally known as the failure envelope, is in the model described as a *bounding line*. At high effective mean stresses the bounding line will coincide with the critical state line. The bounding line as well as the critical state line can be seen in Figure 1, where the bounding line for a dense sample is curved due to the increased peak shear strength.

The path of the bounding line is highly dependent on the void ratio, and therefore the shape of the bounding line is formulated by the *state parameter*, ψ, along with the *critical stress ratio*, M_{cr}. The state parameter in equation (1) is defined as the difference between the current void ratio, e, and the critical void ratio, e_{cr}, and is shown in Figure 2. The state parameter is used in the constitutive model

[1] *M.Sc. Student, Department of Civil Engineering, Aalborg University, Denmark*

[2] *Associate Professor, Department of Civil Engineering, Aalborg University, Denmark*

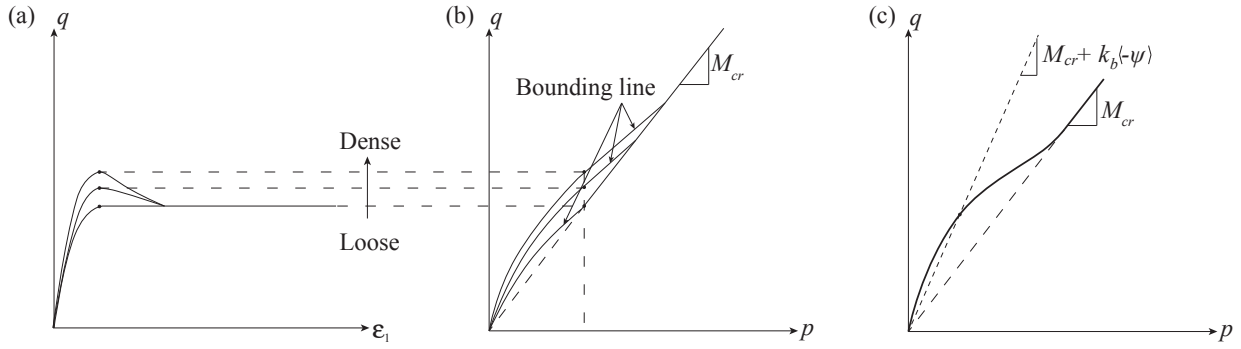

Figure 1: *Peak shear strength (failure envelope) for different deposit densities. (a) $\varepsilon_1 - q$ diagram. (b) $p - q$ diagram (Cambridge diagram). (c) Model formulation of bounding line.*

to prescribe the peak stress level and dilatancy behaviour.

$$\psi = e - e_{cr} \tag{1}$$

The critical stress ratio prescribes the inclination of the critical state line, and is defined as the ratio between the deviatoric and mean stresses, $M_{cr} = q/p$. The critical stress ratio along with the state parameter results in the bounding line, M_b, which is formulated as

$$M_b(\psi) = M_{cr} + k_b \langle -\psi \rangle \tag{2}$$

where k_b is a dimensionless model parameter and $\langle\ \rangle$ is defined as Macauly brackets where $\langle x \rangle = 0$ if $x < 0$ else $\langle x \rangle = x$.

2.2 Characteristic Line

To model the change from compactive to dilative behaviour the use of *characteristic line* is implemented into the model. For monotonic tests this behaviour can be represented by a straight line through origo in p - q space and is independent of relative density (Ibsen, 1998). However, when dealing with cyclic loading a reformulation of the characteristic line is needed because the line is no longer constant and independent of relative density according to Manzari and Dafalias (1997). Therefore the definition of the characteristic line is also formulated by the critical stress ratio and the state parameter, given as

$$M_c(\psi) = M_{cr} + k_c \psi \tag{3}$$

where k_c is a dimensionsless model parameter and the characteristic line is illustrated in Figure 3.

2.3 Stress Dependent Moduli

Both the bulk modulus, K, and the shear modulus, G, are stress dependent, and in order to take this dependency into account, the model uses the following equations

$$K = K_0 \left(\frac{p}{p_{ref}} \right)^b \qquad G = G_0 \left(\frac{p}{p_{ref}} \right)^b \tag{4}$$

where p_{ref} is the reference pressure for which $K = K_0$ and $G = G_0$. The pressure exponent, b, is a model parameter expressing the variation of the elastic modules with the isotropic pressure. The value of b is reported to vary from 0.435, at very

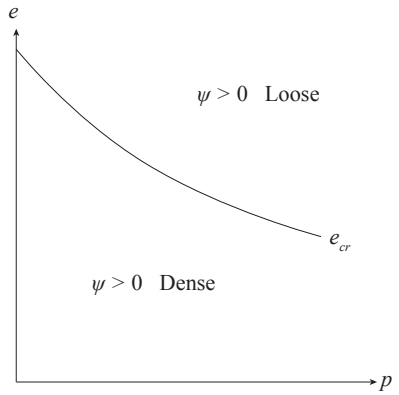

Figure 2: *State parameter used to model peak shear stress and dilatancy behaviour.*

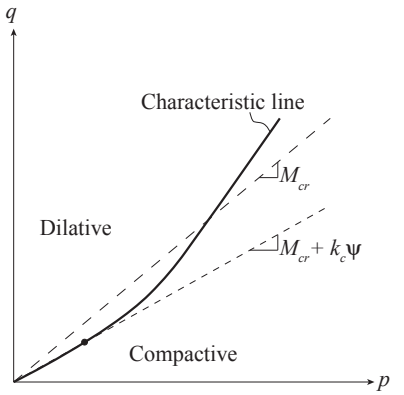

Figure 3: *Characteristic line accounting for the transition from compactive to dilative soil behaviour.*

small strains, to 0.765, at very large strains according to Wroth et al. (1979). A value of 0.5 captures most of the important features of increased shear stiffness with pressure (Wroth and Houlsby, 1985).

2.4 Yield Surface

The constitutive model has its underlying basis in non-associated plasticity and the elastic domain is enclosed by a yield surface with the function given in equation (5). The yield surface has a cone type shape and has its origin positioned in origo, see Figure 4. It should be noted that bold letters characterise tensors and the operators **u**:**v** and $|u|$ refer to the tensor product and tensor norm, respectively. Moreover $p = (\sigma_{11} + \sigma_{22} + \sigma_{33})/3$ and $\boldsymbol{s} = \boldsymbol{\sigma} - p\boldsymbol{I}$ refer to the hydrostatic stress and the deviatoric stress tensor, where $\boldsymbol{I}$ is the identity matrix.

$$f = |\boldsymbol{r}| - \sqrt{\frac{2}{3}} mp \qquad \boldsymbol{r} = \boldsymbol{s} - p\,\boldsymbol{\alpha} \tag{5}$$

The value $\sqrt{\frac{2}{3}}m$ and $\boldsymbol{\alpha}$ define the radius and axis direction of the cone respectively.

The normals to the yield surface, $\partial f/\partial \boldsymbol{\sigma}$, and plastic potential surface, $\partial g/\partial \boldsymbol{\sigma}$, defining the direction of the loading and plastic flow direction are defined as

$$\frac{\partial f}{\partial \boldsymbol{\sigma}} = \boldsymbol{n} - \frac{1}{3} N \boldsymbol{I} \tag{6}$$

$$\frac{\partial g}{\partial \boldsymbol{\sigma}} = \boldsymbol{n} + \frac{1}{3} D \boldsymbol{I} \tag{7}$$

where $\mathbf{n} = \mathbf{r}/|\mathbf{r}|$ is the deviatoric normal to the yield surface as shown in Figure 4. N and D are parameters which determine the magnitude of the isotropic components. The latter is a dilatancy parameter and it controls the isotropic flow direction

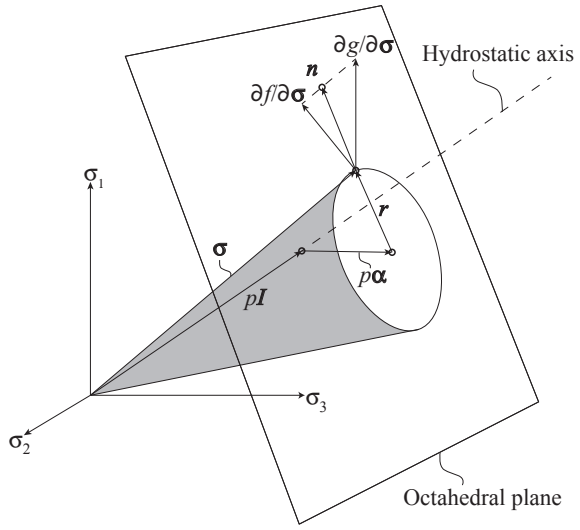

Figure 4: *Illustration of yield surface.*

and thereby the volumetric behaviour of the constitutive model.

2.5 Volumetric Behaviour

The magnitude of the isotropic components can be determined by equation

$$N = \boldsymbol{\alpha} : \boldsymbol{n} + \frac{2}{3} m \tag{8}$$

$$D = (A_0 + A_z)(\boldsymbol{\beta_c} : \boldsymbol{n}) \tag{9}$$

where $A_z = \langle \boldsymbol{z} : \boldsymbol{n} \rangle$ is an unloading dilatancy parameter, which allows the model to take dilatancy during unloading into account and is dependent on the fabric tensor $\boldsymbol{z}$. Furthermore, A_0 is a dimensionless scaling parameter also accounting for dilantancy. The sign of $\boldsymbol{\beta_c} : \boldsymbol{n}$ defines the limit between compressive and dilative behaviour. $\boldsymbol{\beta_c} : \boldsymbol{n} > 0$ indicates stress states inside the characteristic surface and therefore compressive behaviour, whereas loading beyond the characteristic surface gives $\boldsymbol{\beta_c} : \boldsymbol{n} < 0$ and therefore dilative behaviour. The development of the fabric tensor, $\boldsymbol{z}$, is defined by the evolution law

$$d\boldsymbol{z} = \tilde{\boldsymbol{z}} d\lambda \qquad \tilde{\boldsymbol{z}} = -C_z (A_z^{max} \boldsymbol{n} + \boldsymbol{z}) \langle -D \rangle \tag{10}$$

The two parameters C_z and A_z^{max} are positive dimensionless model parameters, and A_z^{max} becomes an upper threshold for A_z. $\boldsymbol{z}$ enables the model to dilate under reversed loading and develop accordingly. $\boldsymbol{z}$ evolves in an opposite direction of $\boldsymbol{n}$ whenever the specimen dilates ($D > 0$) such that the tensor product $\boldsymbol{z} : \boldsymbol{n}$ becomes positive, only when the load direction shifts to unloading.

2.6 Kinematic and Isotropic Hardening

The kinematic evolution law is based on the expression given in equation (11). C_α is a positive model parameter and $b_r = 2\sqrt{2/3}(M_b - m)$ and must abide $b_r > |\boldsymbol{\beta_b} : \boldsymbol{n}|$. The rate of evolution will converge to zero as $\boldsymbol{\alpha}$ approaches the bounding surface which implies that the stress state remains inside the bounding surface during hardening.

$$d\boldsymbol{\alpha} = \tilde{\boldsymbol{\alpha}} d\lambda \qquad \tilde{\boldsymbol{\alpha}} = C_\alpha \left(\frac{|\boldsymbol{\beta_b} : \boldsymbol{n}|}{b_r - |\boldsymbol{\beta_b} : \boldsymbol{n}|} \right) \boldsymbol{\beta_b} \tag{11}$$

The size of the plastic multiplier, $\Delta\lambda$, can be determined from equation

$$\Delta\lambda = \frac{f(\boldsymbol{\sigma})}{\partial f/\partial \boldsymbol{\sigma} : \boldsymbol{C} : \partial g/\partial \boldsymbol{\sigma} + H} \tag{12}$$

where $\boldsymbol{C}$ is the hypoelastic constitutive matrix and H is the hardening module, which is determined from

$$H = p \left(\boldsymbol{n} : \tilde{\boldsymbol{\alpha}} + \sqrt{\frac{2}{3}} \tilde{m} \right) \tag{13}$$

2.7 Multi-axial Formulation

Granular materials are strongly dependent on the third deviatoric stress invariant, which can be proven by comparing triaxial compression and extension tests, which shows that a lower shear strength can be sustained in triaxial extension. In order to account for the third stress invariant and thereby a more correct behavioural simulation of granular materials, the bounding and characteristic lines are reformulated into bounding and characteristic surfaces defined in a multi-axial stress space. The bounding and characteristic surfaces are described by a versatile shape function, $g(c,\theta)$, which was first presented by Krenk (1996). The formulation is based on the second, J_2, and third, J_3, deviatoric stress invariants and the Lode angle, θ. The shape function is defined as

$$g(c,\theta) = \frac{\cos(\gamma)}{\cos\left(\frac{1}{3}\arccos\left(\cos(3\gamma)\cos(3\theta)\right)\right)} \tag{14}$$

$$\gamma = \frac{\pi}{3} + \arctan\left(\frac{1-2c}{\sqrt{3}}\right) \tag{15}$$

$$\cos(3\theta) = \frac{3\sqrt{3}}{2}\frac{J_3}{(J_2)^{\frac{3}{2}}} \tag{16}$$

The shape parameter, c, can attain any value between 0.5 and 1. A value equal to 1 produces a circular surface contour in the octahedral plane and a value of 0.5 produces a triangle. Any value in between creates a cross between the two shapes as seen in Figure 5.

2.8 Image Points

The constitutive model is formulated by applying image points, $\boldsymbol{\alpha}_i$, which defines points on a surface in the octahedral plane, pointing from the hydrostatic axis to the image point in the direction of $\mathbf{n}$, see equation (17) and Figure 6. These image points are used in the formulation to model dilatancy and the evolution laws for hardening parameters.

$$\boldsymbol{\alpha}_i = \sqrt{\frac{2}{3}}\left(g(c_i,\theta_{\boldsymbol{n}})M_i(\psi) - m\right)\boldsymbol{n}, \quad i = b,c \tag{17}$$

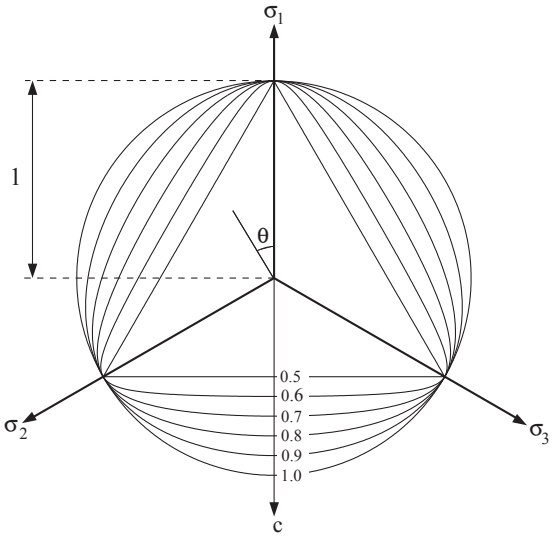

Figure 5: *Family of shape contours prescribed by the shape function $g(c,\theta)$.*

3 Integration Scheme

When an integration scheme is used the infinitesimal changes, $d\boldsymbol{\sigma}$, now becomes finite, $\Delta\boldsymbol{\sigma}$. This implies that the constitutive relation can be expresses as

$$\Delta\boldsymbol{\sigma}_{j+1} = \boldsymbol{D}^{ep}(\boldsymbol{\sigma}_j)\,\Delta\,\boldsymbol{\varepsilon}_{j+1} \tag{18}$$

The Forward Euler integration scheme is choosen, of which the principles for updating the stress tensor can be expressed as

$$\boldsymbol{\sigma}_{j+1} = \boldsymbol{\sigma}_j + \Delta\boldsymbol{\sigma}_{j+1} \tag{19}$$

This implies that the stress increment, $\Delta\boldsymbol{\sigma}$, only depends on the previous stress state j. This is problematic as the scheme may lead to stresses outside the yield surface, which can not exist. In the Forward Euler integration scheme these errors are not corrected. Errors may therefore accumulate and stresses drift away from the yield surface, as more steps are taken, as illustrated in Figure 7. When the step length is reduced the error is reduced as well, hence this method demands a relative small step length, which require a lot of computational power (Krabbenhøft, 2002).

3.1 Implementation strategy

In general the course of action regarding the implementation of the model is outlined in Table 1, where $\mathbf{D}^*$ is either the elastic, $\mathbf{D}^{el}$, or elasto-plastic, $\mathbf{D}^{ep}$, constitutive tensor dependent on elastic or plastic material response.

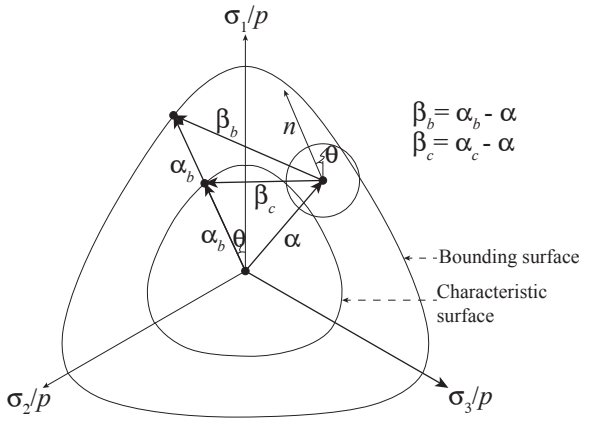

Figure 6: *Illustration of bounding, characteristic and yield surface in the octahedral plane.*

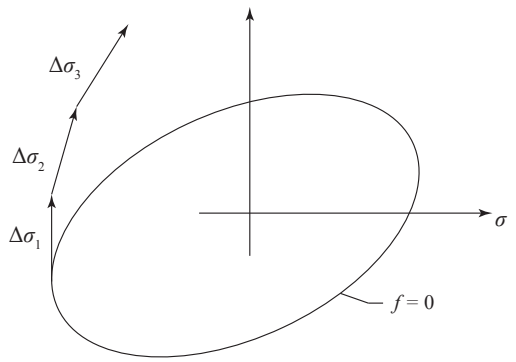

Figure 7: *Illustration of errors by using the Forward Euler integration scheme. (Krabbenhøft, 2002)*

Table 1: *Procedure regarding the implementation of the Forward Euler integration scheme to the modified two-surface elasto-plasticity model.*

Modified Manzari (Forward Euler)

Initial state:
$\boldsymbol{\alpha_0}$, c_b, c_c, b, G_0, K_0, p_{ref}
m_0, A_0, A_z, $\mathbf{z}$, C_z, A_z^{max}, C_α, $\mathbf{D}_0^*$

Iterations $i = 1, 2, ..., i_{max}$
Given parameters: $\Delta\varepsilon_{1,i}$, $\Delta\sigma_{2,i}$, $\Delta\sigma_{3,i}$

Calculate unknown stresses and strains from $\mathbf{D}^*$:
$\Delta\varepsilon_{3,i}$, $\Delta\varepsilon_{2,i}$, $\Delta\sigma_{1,i}$

Determine hydrostatic-, deviatoric stress and yield function:
$\mathbf{s}$, p, $\mathbf{r}$, $f(\boldsymbol{\sigma})$

if $f(\boldsymbol{\sigma}) < 0$
$\mathbf{D}^* = \mathbf{D}^{el}$

else:
θ, γ, g, M_b, M_c, α_b, α_c, β_b, β_c, N, $\frac{\partial f}{\partial \boldsymbol{\sigma}}$, A_z, D_{dil}, $\tilde{\boldsymbol{z}}$, $\frac{\partial g}{\partial \boldsymbol{\sigma}}$, $\Delta\lambda$, $\tilde{\boldsymbol{\alpha}}$

$$\mathbf{D^*} = \mathbf{D^{ep}} = \boldsymbol{D} - \frac{\boldsymbol{D}\frac{\partial g}{\partial \boldsymbol{\sigma}}\frac{\partial f}{\partial \boldsymbol{\sigma}}^T\boldsymbol{D}}{H + \frac{\partial f}{\partial \boldsymbol{\sigma}}^T\boldsymbol{D}\frac{\partial g}{\partial \boldsymbol{\sigma}}}$$

Update Variables:
$\boldsymbol{\alpha} = \boldsymbol{\alpha} + \Delta\lambda\tilde{\boldsymbol{\alpha}}$
$\mathbf{z} = \mathbf{z} + \Delta\lambda\tilde{\mathbf{z}}$

end

4 Efficiency, Accuracy and Stability

The Forward Euler integration scheme is evaluated on efficiency, accuracy and stability to evaluate the performance and determine if the integration scheme in Table 1 is applicable for this particular model. Simulations of drained monotonic and cyclic tests are performed for the analysis. The adopted model parameters are based on the original formulation of the constitutive model by Manzari and Dafalias (1997) and can be seen in Table 2.

Table 2: *Model parameters adopted for analysis of efficiency, accuracy and stability.*

K_0=31.4 MPa	M_c=1.1	k_b=4.0	A_0=2.64
G_0=31.4 MPa	λ=0.025	k_c = 4.2	A_z^{max}=100
	e_r=0.93	C_α=1200	C_z=100

Both the monotonic and cyclic tests simulates a medium-dense sample with a mean stress of $p = 60$ kPa with ε_1 ranging from 0 - 10 %. The simulations are illustrated in Figures 8 and 10. To evaluate the accuracy of the integration scheme an error measure is used, defined by

$$error = \frac{1}{N}\sum_{i=1}^{N}\frac{|\boldsymbol{\sigma}_i - \boldsymbol{\sigma}_{i,exact}|}{\boldsymbol{\sigma}_{i,exact}} \tag{20}$$

where N is the number of steps and $\boldsymbol{\sigma}_{i,exact}$ refers to the exact solution approximated by simulations having a very small step size and where convergence has occurred. The accuracy is measured as a function of the imposed strain increments, $\Delta\varepsilon_1$. The results are listed in Table 3.

Table 3: *Results from accuracy analysis of the Forward Euler integration scheme, applied at the Modified Critical State Two-Surface model (1-6) and a Drucker Prager model with non linear isotropic hardening (DP1-DP4).*

No.	Loading	N	$\Delta\varepsilon_1$	Error [%]
1	Monot.	10,000	10^{-5}	21.41
2	Monot.	100,000	10^{-6}	13.39
3	Monot.	1,000,000	10^{-7}	1.18
4	Cyclic	10,000	10^{-5}	42.05
5	Cyclic	100,000	10^{-6}	22.71
6	Cyclic	1,000,000	10^{-7}	Unstable
DP1	Monot.	10	10^{-2}	2.24
DP2	Monot.	100	10^{-3}	0.26
DP3	Monot.	1000	10^{-4}	0.07
DP4	Monot.	10000	10^{-5}	0.01

4.1 Monotonic CD Response

For the monotonic simulations a triaxial compression test has been simulated. A convergence analysis proved that an accurate simulation is performed with an increment in the order of $\Delta\varepsilon_1 = 10^{-8}$, which is a rather small increment size and therefore demands relatively large computational costs at the expense of efficiency. Larger increments have been attempted to improve the efficiency, but the approximated solution diverges too far away from the exact solution and the error becomes too large, as seen in Table 3.

The convergence rate for the Modified Critical State Two-Surface model is compared with a Drucker Prager constitutive model with nonlinear isotropic hardening, where the Forward Euler integration scheme also is applied. The ε_1 - q diagram is depicted in Figure 9, and the relative error is given in Table 3. From this it is seen that convergence is reached with a step length of 10^{-3} to 10^{-4}, which is much faster than the Modified Critical State Two-Surface model, which need increments smaller than 10^{-7} to obtain convergence. This indicate that when the complexity of a constitutive model increases, the needed step size and thereby the usability of the Forward Euler integration scheme decreases. This makes the importance of return mapping more relevant, when constitutive models becomes more complex.

4.2 Cyclic CD Response

When simulating cyclic response the model shows reasonably good stress-strain behaviour, as seen in Figure 10. As with the monotonic simulation the accuracy increases with decreasing strain increments. However, at some point the increments become too small and produce a problem with stability in the model. As seen in Table 3, when the strain increments becomes $\Delta\varepsilon_1 = 10^{-7}$ the model becomes unstable. This makes it difficult to estimate the error of the different strain increments because convergence has not been established. The error measures have therefore been compared to the last stable increment size, which is $\Delta\varepsilon_1 = 0.5\times10^{-6}$. This means that the calculated error for the cyclic simulations must be considered with a high amount of uncertainty.

However, the instability problems that the model faces during cyclic loading indicates that there is a problem with the implementation of the integration scheme into the constitutive model. Instability problems does not make physical sense when reducing the increments, because a reduction of the increment size will entail a solution approaching the exact value.

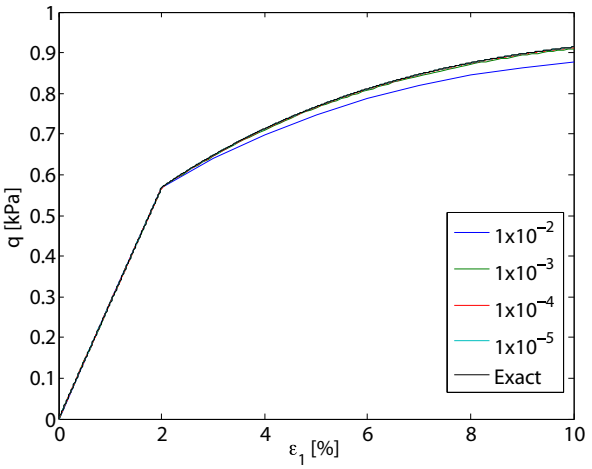

Figure 9: *Results of monotonic simulation with Drucker Prager model with nonlinear isotropic hardening and the accuracy of different strain increments.*

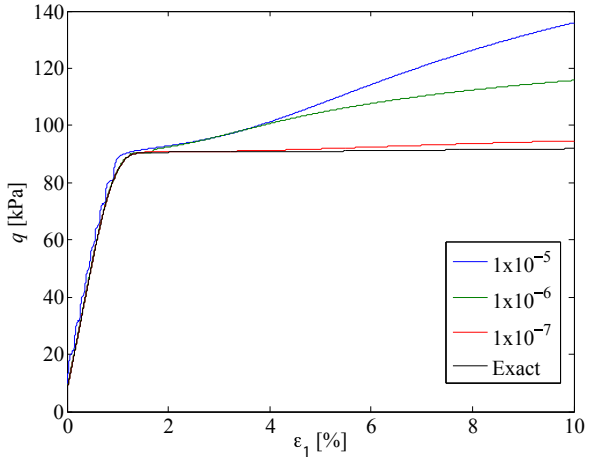

Figure 8: *Results of monotonic simulation with Modified Critical State Two-Surface model and the accuracy of different strain increments.*

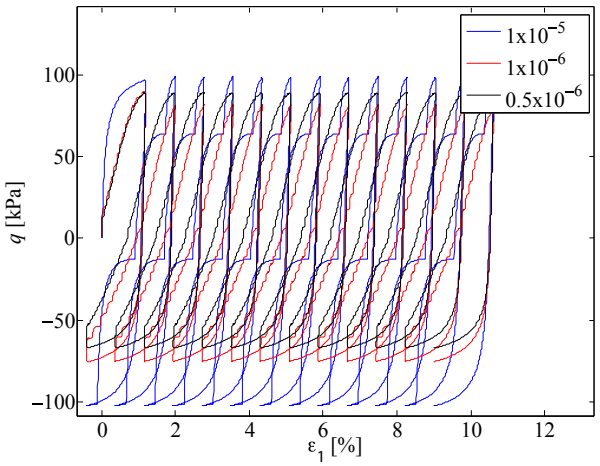

Figure 10: *Results of cyclic simulation and the accuracy of different strain increments.*

5 Conclusion

The Forward Euler integration scheme is implemented into the Modified Critical State Two-Surface model originally formulated by Manzari and Dafalias (1997) and modified by LeBlanc (2008). The objective was to investigate if a simple integration scheme could be implemented into an advanced constitutive model and still model correct stress-strain behaviour of a cohesionless soil. Monotonic and cyclic simulations are performed on a medium-dense sand in order to measure the accuracy of the integration scheme for different strain increments. It is found that with the Forward Euler method the step size will be inappropriately small ($\Delta\varepsilon_1 < 10^{-7}$) for monotonic loading. More importantly the model becomes unstable for cyclic loading, thereby inducing a large inaccuracy into the model. However, this is not believed to be a problem with the integration scheme itself, but the implementation of the constitutive model. Still, the conclusion is that a simple integration scheme, such as the Forward Euler method, can not be recommended for a model of this complexity.

References

Ibsen, **1998**. Lars Bo Ibsen. *The Mechanism Controlling Static Liquefaction and Cyclic Strength of Sand.* Proc. Int. Workshop on Physics and Mechanics of Soil Liquefaction, A. A Balkema, Rotterdam, (27), pages 29–39, 1998.

Krabbenhøft, **2002**. Kristian Krabbenhøft. *Basic Computational plasticity*, 2002.

Krenk, **1996**. S. Krenk. *Family of Invariant Stress Surfaces.* Journal of Engineering Mechanics - Proceedings of the ASCE, Vol. 122(3), pages 201–208, 1996.

LeBlanc, **2008**. Christian LeBlanc. *A modified critical state two-surface plasticity model for sand - theory and implementation.* ISSN: 1901-7278, DCE Technical Memorandum no. 8. Aalborg University, 2008.

Manzari and Dafalias, **1997**. M.T. Manzari and Y.F. Dafalias. *Critical state two-surface plasticity model for sands.* Géotechnique, Vol. 47(2), pages 255–272, 1997.

Schofield and Wroth, **1968**. A.N. Schofield and C.P. Wroth. *Critical State Soil Mechanics.* ISBN: 978-0641940484. McGraw-Hill, 1968.

Wroth and Houlsby, **1985**. C.P. Wroth and M.F. Houlsby. *Soil mechanics: property characterisation and analysis procedures.* Proc. 11th International Conf. Soil Mech. Found. Engng. San Fransisco, pages 1–50, 1985.

Wroth, Randolph, Houlsby, and Fahey, **1979**. C.P. Wroth, M.F. Randolph, G.T. Houlsby, and M. Fahey. *A review of the engineering properties of soils with particular reference to the shear modulus.* Tech. Report CUED/D-SOILS TR75. University of Cambridge, 1979.